Variable stoichiometry in Sb-induced (2×4) reconstructions on GaAs(001)

Akihiro Ohtake*
National Institute for Materials Science (NIMS), Tsukuba 305-0044, Japan

Motoi Hirayama, Jun Nakamura, and Akiko Natori
Department of Electronic-Engineering, The University of Electro-Communications (UEC-Tokyo), Chofu, Tokyo 182-8585, Japan

(Received 6 May 2009; revised manuscript received 23 November 2009; published 23 December 2009)

The structure and composition of Sb-induced (2×4) reconstructions on the GaAs(001) surface have been systematically studied using scanning tunneling microscopy, reflectance-difference spectroscopy, x-ray photoelectron spectroscopy, reflection high-energy electron diffraction, and first-principles calculations. We show that several types of Sb-induced (2×4) reconstructions are formed, depending on the Sb coverage. The (2×4) surface with low Sb coverages has the structure with only one anion dimer at the outermost layer. For the Sb-rich (2×4) phase, on the other hand, we propose the structure model consisting of anion dimers at the first and third layers and three-coordinated As atoms at the second layer.

DOI: 10.1103/PhysRevB.80.235329 PACS number(s): 68.35.B−, 68.37.Ef, 61.05.jh

I. INTRODUCTION

The adsorption of group-V atoms on (001) surfaces of III-V compound semiconductors is technologically important for the fabrication of heterostructures based on III-V semiconductors. In particular, the interaction of Sb with the GaAs(001) surface has been the subject of a number of experimental and theoretical investigations. A variety of reconstructions, such as (2×8), (1×3), and (2×4) are formed on the Sb-terminated GaAs(001) surface.[1,2] Among these reconstructions, the atomic geometry of (2×4) has been most extensively studied. It has been well established that the (2×4) reconstructions, which are usually observed on the GaAs and InAs surfaces, are not formed on InSb and GaSb surfaces. Thus, the structure identification of the Sb-induced (2×4) reconstruction is a key to understand the group-V rich surface reconstructions of III-V semiconductors.

On the basis of photoelectron spectroscopy measurements, Madea *et al.* proposed the structure model built up with three Sb dimers on the Ga-terminated GaAs(001) surface for the Sb-induced (2×4) reconstruction [Fig. 1(a)].[1] While this structure model has been later supported by x-ray standing wave measurements,[3] first-principles calculations have shown that the three Sb-dimer structure is energetically unfavorable.[4,5] Esser *et al.* proposed the α_2 model [Fig. 1(d)] on the basis of tight-binding calculations and a comparison of measured and calculated reflectance difference spectra.[4] On the other hand, scanning tunneling microscopy (STM) observations by Moriarty *et al.* revealed the (2×4) unit with only one Sb dimer at the outermost layer [Fig. 1(e)].[6] The one-Sb-dimer structures, which are now referred to as the δ structures, have been supported by the first-principles calculations by Schmidt and Bechstedt: while the $\beta 2_3$ structure [Fig. 1(b)] is stable under the extremely Sb-rich condition, δ_1 [Fig. 1(e)] and δ_2 [Fig. 1(f)] structures become more favorable under more Ga-rich conditions.[5] Although recent STM and photoelectron spectroscopy experiments supported the δ_2 model,[7] STM images incompatible with the δ_1/δ_2 models have been also reported.[8,9] Judging from these results, it appears that the structure identification of the Sb-induced GaAs(001)(2×4) surface is not fully convincing.

This paper reports a systematic study on the (2×4) reconstructions formed by the adsorption of Sb on GaAs(001) using reflection high-energy electron diffraction (RHEED), reflectance-difference spectroscopy (RDS), x-ray photoelectron spectroscopy (XPS), STM, and first-principles calculations. We carefully controlled the coverage of Sb on the GaAs(001) surface, and found that there exist several types of (2×4) reconstructions. We show that the (2×4) surface with low Sb coverages has the δ-type structure, in good

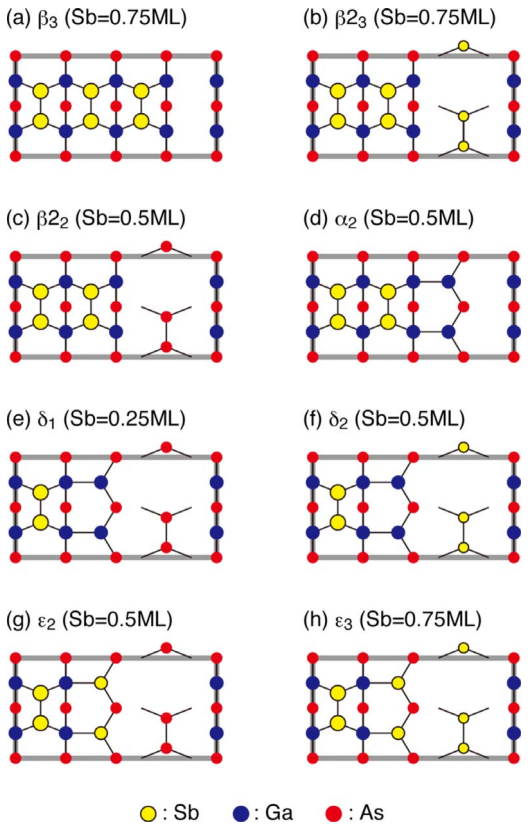

FIG. 1. (Color online) Structure models for the GaAs(001)−(2×4) surface. Large, middle, and small circles indicate top-, second-, and third-layer atoms, respectively.

agreement with the results in Refs. 5–7. On the other hand, none of the structure models shown in Figs. 1(a)–1(f) could account for the experimental data from the (2×4) surface with higher Sb coverages. We propose a structure model consisting of anion dimers at the first and third layers and three-coordinated As atoms at the second layer.

II. EXPERIMENTAL

The experiments were performed in a system of interconnecting ultrahigh vacuum (UHV) chambers for molecular-beam epitaxy (MBE) growth and for on-line surface characterization by means of STM and XPS.[10] All the STM images were acquired at room temperature using electrochemically etched tungsten tips. XPS measurements were carried out by using monochromatic Al Kα radiation (1486.6 eV). Photoelectrons were detected at an emission angle of 10° from the surface. The RD spectra were obtained using a modified Jobin Yvon RD spectrometer. The RDS results are commonly displayed in terms of $\Delta\tilde{r}/\tilde{r}=(\tilde{r}_{1\bar{1}0}-\tilde{r}_{110})/\tilde{r}$, where $\tilde{r}_{1\bar{1}0}$ and $\tilde{r}_{110}$ are the near-normal-incidence complex reflectances for light linearly polarized along $[1\bar{1}0]$ and [110], respectively. We present only the data in the form $\Delta r/r=\mathrm{Re}(\Delta\tilde{r}/\tilde{r})$.

Nondoped and nominally on-axis GaAs(001) substrates were used for the RHEED, RDS, and XPS measurements, while the Si-doped ($N\approx1-4\times10^{18}$ cm^{-3}) substrates were employed for the STM experiments. Cleaned GaAs(001)$-(2\times4)$ surfaces were first obtained by growing an undoped homoepitaxial layer (~0.5 μm) on a thermally cleaned GaAs(001) substrate. The GaAs(001)$-(2\times4)$ surfaces were kept at 440 °C in a good UHV condition of $\sim5\times10^{-11}$ Torr, and then exposed to an Sb_4 flux with a beam-equivalent pressure of 1×10^{-8} Torr. To control the Sb coverage on the GaAs(001) surface, the substrate temperature was changed between 440 °C and 640 °C in steps of 20 °C. RHEED and RDS measurements were carried out at each step, first with the Sb flux and then without the Sb flux, and the temperature was kept until the RD intensities were saturated in either case. After the measurements were completed at a given temperature, the surfaces were exposed to the Sb flux again and then the temperature was increased or decreased to the next step.

III. CALCULATIONS

First-principles calculations,[15,16] based on the density functional theory[14] with the generalized gradient approximation,[17] were performed. A slab geometry was used for the simple calculation, which has the supercell consisting of seven atomic layers and of vacuum region (12 Å in thickness). The back side of the slab is terminated with 16 fictitious H atoms which eliminate artificial dangling bonds and prevent it from coupling with the front side. The wave functions were expanded in plane waves with a kinetic energy cutoff of 16 Ry. Four k points in the irreducible Brillouin zone of the (2×4) surface were used for the integration in k space. The top six layers were relaxed until all the forces were less than 0.5 eV/nm.

The stability of a certain structure in the equilibrium can be determined from the surface free energy and the chemical potentials μ_i of the surface constituents i=Ga, As, and Sb.[5] In the present study, the surface formation energy ΔE_{surf} is defined as

$$\Delta E_{\mathrm{surf}}=E_{\mathrm{tot}}-E_{\mathrm{ref}}-n_{\mathrm{Ga}}\mu_{\mathrm{Ga}}-n_{\mathrm{As}}\mu_{\mathrm{As}}-n_{\mathrm{Sb}}\mu_{\mathrm{Sb}}, \quad (1)$$

where E_{tot} is the total energy of the Sb-induced (2×4) reconstruction, E_{ref} is taken as the total energy of the clean GaAs(001)$-\beta2(2\times4)$ surface, and n_i are the difference in the number of the atomic species i=Ga, As, and Sb between Sb-stabilized and As-stabilized (2×4) structures. The chemical potentials μ_i are expressed as $\mu_i=\mu_i^{\mathrm{bulk}}+\Delta\mu_i$, and it holds that

$$\Delta\mu_{\mathrm{Ga}}+\Delta\mu_{\mathrm{As}}=\mu_{\mathrm{Ga}}+\mu_{\mathrm{As}}-\mu_{\mathrm{Ga}}^{\mathrm{bulk}}-\mu_{\mathrm{As}}^{\mathrm{bulk}}=\Delta H_f(\mathrm{GaAs}), \quad (2)$$

where ΔH_f(GaAs) is the formation enthalpy of GaAs.

IV. RESULTS AND DISCUSSION

We first examined whether the atomic structure of the Sb-induced (2×4) reconstruction changes with the preparation conditions using RHEED and RDS. When the GaAs(001)$-(2\times4)$ surface was exposed to the Sb flux at 440 °C, (2×8) RHEED patterns appeared. As the temperature was increased, the (2×8) reconstruction changed to the (2×4) one at 520 °C. The (2×4) reconstructions are observed in relatively wide temperature ranges of 520–640 °C and 480–620 °C with and without Sb fluxes, respectively. When the Sb flux was interrupted at 640 °C, the $c(8\times2)$ RHEED patterns were observed, suggesting that Sb was completely desorbed.

Figure 2(a) shows RD spectra obtained from GaAs(001) surfaces under the Sb_4 flux of 1×10^{-8} Torr. The solid and dashed curves were measured when the substrate temperature was increased and decreased, respectively. The shape of the RD spectrum significantly changes in the temperature range of 520–640 °C, where (2×4) RHEED patterns were observed. Specifically, a negative feature at ~1.8 eV and a broad positive feature at ~3.9 eV in the spectrum measured at 520 °C are shifted by ~0.2 eV to higher energy as the substrate temperature is increased. The observed peak shift is in the opposite direction to those in the optical transition energies in GaAs.[11] Thus, the present result could not be explained by the temperature dependence of optical transition energies. These results indicate that the Sb-adsorbed (2×4) surface changes its structure and/or composition depending on the substrate temperature. Similar changes in RD spectra were observed in RD spectra measured without the Sb flux [Fig. 2(b)]. The spectra measured at 640 °C and 560 °C with the Sb flux [Fig. 2(a)] resemble those at 560 °C and 480 °C without the Sb flux [Fig. 2(b)], respectively. As we will show later, the amount of Sb atoms on the GaAs(001) surface decreases with increasing substrate temperature. Thus, the supply of the Sb flux compensates for the desorption of Sb from the (2×4) surface at temperatures higher by ~80 °C. As can be seen in Figs. 2(a) and 2(b), no

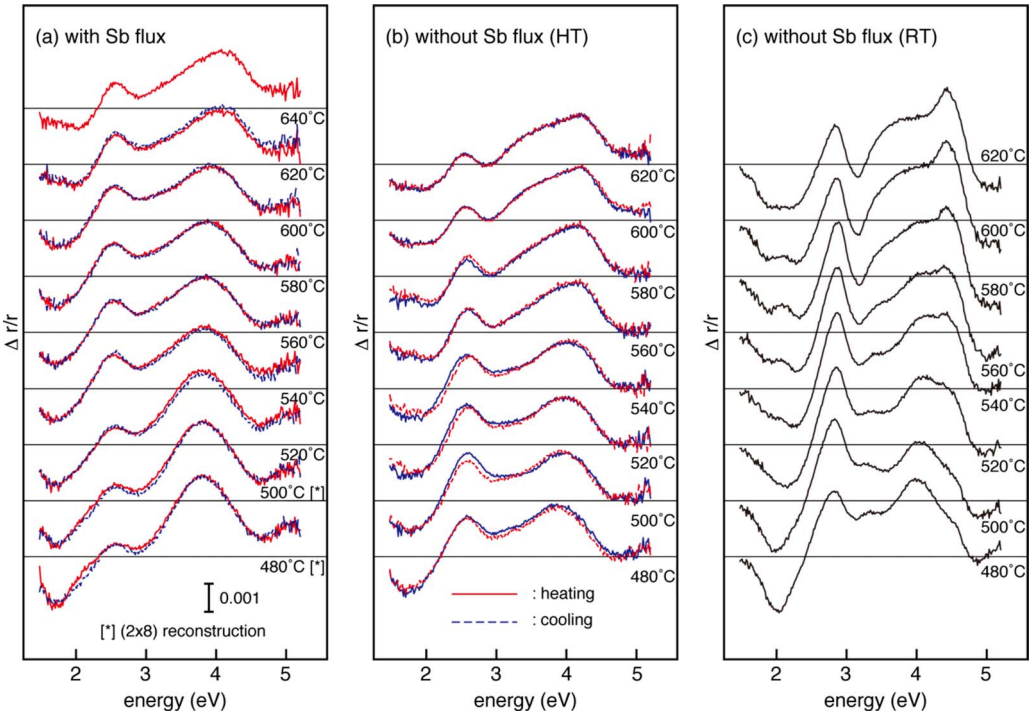

FIG. 2. (Color online) RD spectra measured from the Sb-adsorbed GaAs(001)−(2×4) surfaces (a) with and (b) without the Sb_4 flux of 1×10^{-8} Torr. Solid (dashed) curves are measured when the substrate temperature was increased (decreased) from 440 °C (640 °C). (c) RD spectra measured after the sample was cooled to room temperature.

hysteresis was observed, indicating that the structure change is reversible.

Shown in Fig. 2(c) are the spectra measured after the sample was cooled to room temperature. While a small blue shift of about 0.2 eV, together with sharpened and increased anisotropies, occurs, the overall line shapes of the room-temperature spectra are very similar to the corresponding high-temperature ones. In addition, fine structures are clearly observed at room temperatures. For example, the positive feature develops at 4.4 eV as the temperature is increased [Fig. 2(c)], which is observed as a peak shift in Fig. 2(b), as mentioned above. Thus, it is suggested that there exist more than one (2×4) phase, the ratio of which varies as a function of substrate temperature.

In order to obtain details of the structure change, the samples were transferred from MBE chamber into another UHV chambers for STM and XPS measurements. For this purpose, the samples were quenched after the RDS and RHEED measurements without the Sb flux at given temperatures. Figure 3 shows photoelectron intensity ratios of As 3*d*/Ga 3*d* and Sb 4*d*/Ga 3*d* measured from the Sb-adsorbed GaAs(001) surfaces. The changes in photoelectron intensities are reversible, being consistent with the RDS results [Fig. 2(b)]. The Sb/Ga ratio decreases with increasing temperature by a factor of three, indicating that the saturation coverage of Sb in the (2×4) reconstruction changes with substrate temperature. Another noteworthy finding is that the Ga/As ratios remain almost constant in the whole range of substrate temperature: the change in the As coverage is estimated to be below 0.2 ML. Since Ga atoms are hardly desorbed below 640 °C, the present result shows that the desorption of As is negligible. From these results, we conclude that the structure change in (2×4) reconstruction is closely related with the adsorption/desorption of Sb and is not accompanied by the drastic change in the surface As coverage.

Figures 4(a)–4(d) show filled-state STM images taken from the Sb-induced (2×4) surfaces prepared at 480, 520, 560, and 600 °C. The (2×4) unit cells observed in these images can be classified into types A, B, and C, as indicated in the figure. The type-A feature is interpreted as the unit cell having two anion dimers at the surface layer. Although several possible structure models, such as $\beta2_3$ [Fig. 1(b)], $\beta2_2$ [Fig. 1(c)], and α_2 [Fig. 1(d)], could account for the type-A

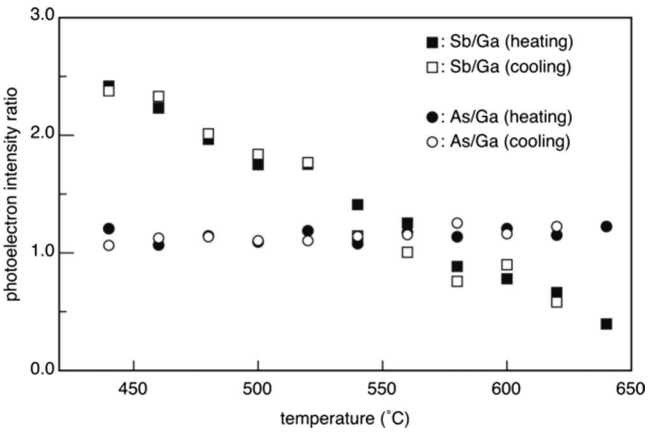

FIG. 3. Photoelectron intensity ratios of As 3*d*/Ga 3*d* (circles) and Sb 4*d*/Ga 3*d* (squares) plotted as a function of substrate temperature. Open and closed symbols correspond to the data obtained from the samples prepared by increasing and decreasing the substrate temperature, respectively.

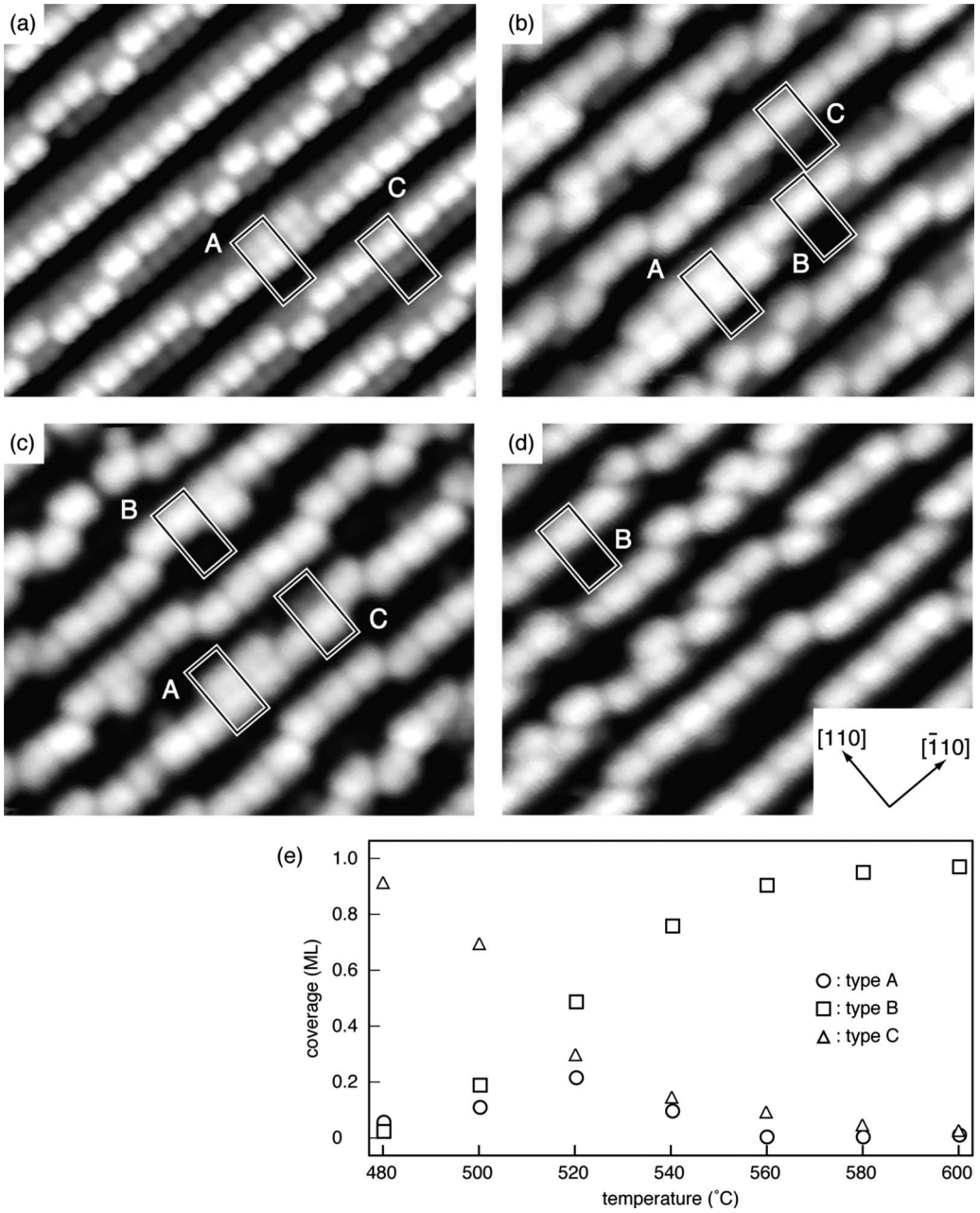

FIG. 4. Filled-state STM images obtained from the Sb-induced (2×4) reconstructions prepared at 480 °C (a), 520 °C (b), 560 °C (c), and 600 °C (d). Image dimensions are 80 Å$\times$96 Å. The images were taken with a sample bias of −2.5 V. (e) Relative coverages of types-A, -B, and -C units plotted as a function of the preparation temperature.

feature, further studies are needed to determine the atomic geometry of the type-A feature.

Previous first-principles calculations[4,5] have predicted that the $\beta2_3$ structure is stable under Sb-rich conditions. However, as shown in Fig. 4(e), where relative coverages of types-A, -B, and -C units are plotted as a function of the temperature, the majority of the (2×4) unit cells have type-C features (~90% in coverage), and the density of the (2×4) unit with the type-A feature is less than 5% on the most Sb-rich (2×4) surface [Fig. 4(a)] prepared at 480 °C. On the other hand, type-B units are dominant on the surface prepared at 600 °C [Fig. 4(d)] (~95%).

As shown in Figs. 5(a) and 5(b), the types-B and -C features could be distinguished within the trenches between top-layer dimer rows: bright features corresponding to the atoms at the second layer are clearly seen in type-C units. Since cation atoms are hardly imaged in filled-state STM images, the type-B features are interpreted in terms of δ_1/δ_2 models. Shown in a part of Figs. 5(e) and 5(f) are topographic line profiles for the types-B and -C features, respectively. While shoulders are clearly seen at ~1.5 Å lower from the outermost surface in Fig. 5(f), such characteristic features are not present in Fig. 5(e). Since the height difference between the first and second layers is ~1.4 Å, it is likely that anion

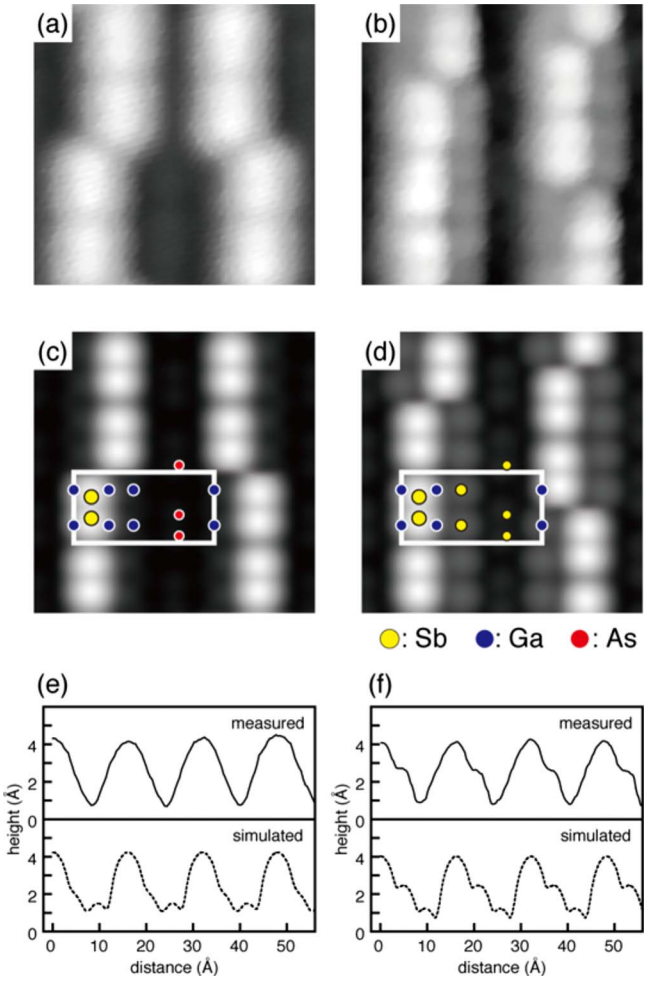

FIG. 5. (Color online) Filled-state STM images obtained from the Sb-induced (2×4) surface prepared at 560 °C (a) and 480 °C (b). The images were taken with a sample bias of −2.5 V. Simulated STM image of the δ_1 (c) and ε_3 (d) models using a filled state bias of 2 V below the valence band maximum. The image dimension is 32 Å×32 Å. Solid curves in (e) and (f) show the topographic line profiles for the sample prepared at 560 °C and 480 °C, respectively, in the [110] direction. Dotted curves are obtained from the simulated images for the δ_1 (e) and ε_3 (f) models.

atoms at the second layer are observed as shoulders in Fig. 5(f). Thus, for the type-C features, we proposed structure models shown in Figs. 1(g) and 1(h), which are denoted by ε structures. This ε structure results from the replacement of the three-coordinated Ga atom at the second layer of the δ structure by the Sb atom, and agrees with the electron counting heuristics.[12]

Figures 5(a)–5(d) compares the measured and simulated STM images. Simulated images were extracted from first-principles calculations: after structural relaxation, extracting isocontour surfaces of a suitably defined local density of states generated numerically simulated constant current STM images. For the Sb-deficient (2×4) structure [Figs. 5(a) and 5(b)], the observed STM image could be well reproduced either by δ_1 [Fig. 1(e)] or δ_2 [Fig. 1(f)] models. On the other hand, ε_2 [Fig. 1(g)] and ε_3 [Fig. 1(h)] models could account for the observed features of the Sb-rich (2×4) surface: as

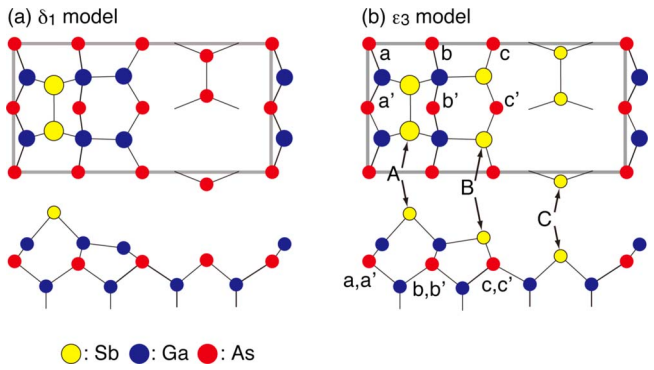

FIG. 6. (Color online) Optimized δ_1 (a) and ε_3 (b) models.

shown in Figs. 5(c) and 5(d), bright features corresponding to the three-coordinated anion atoms at the second layer are clearly observed in both observed and calculated images. In addition, the topographic line profile (solid curve) in Fig. 5(f) is quite similar to that simulated from the ε_2 and ε_3 models (dotted curve). Our analysis, however, still remains to assign the anion atom to As and Sb atom types, because Sb and As atoms in the δ- and ε-type structures were hardly distinguished in simulated STM images.[13]

The Sb coverages of the δ_1, δ_2, ε_2, and ε_3 structures are 0.25, 0.5, 0.5, and 0.75 ML, respectively. Since, as discussed earlier, our XPS analysis show that the amount of Sb atoms in the (2×4) structure at 480 °C is three times larger than that at 600 °C, the δ_1 (Sb=0.25 ML) and ε_3 (Sb =0.75 ML) models are suggested for the less and more Sb-rich (2×4) structures. In addition, both δ_1 and ε_3 models contain 0.25 ML of As, which is consistent with the XPS result: the As/Ga XPS intensity ratio for the Sb-deficient (2×4) surface nearly equals the value for the Sb-rich one. At this stage, therefore, the δ_1 and ε_3 models can be proposed as possible candidates for the Sb-deficient and Sb-rich (2×4) surfaces, respectively. Here, we note that our first-principles calculations and RHEED rocking-curve analysis suggested the possible coexistence of Sb-Sb, As-As, and Sb-As dimers in the Sb-induced (2×4) reconstruction, as we will show later part in this paper. This means that various combinations of Sb-Sb, As-As, and Sb-As dimers in the δ- and ε-type structures could also results in the measured XPS intensity ratio and that further studies are needed to assign atomic species of anion atoms.

We have examined the relative stability of the δ_1 [Fig. 6(a)] and ε_3 [Fig. 6(b)] models. Because of the different numbers of Sb and Ga atoms per unit cell, the comparison of the total energies for different models has to take into account the chemical potentials of Sb [$\Delta\mu$(Sb)] and Ga [$\Delta\mu$(Ga)]. The phase diagram in dependence upon $\Delta\mu$(Sb) and $\Delta\mu$(Ga) is shown in Fig. 7(a). The δ_1 structure is the most stable for lower $\Delta\mu$(Sb) and higher $\Delta\mu$(Ga), in good agreement with the results in Ref. 5. On the other hand, for higher $\Delta\mu$(Sb) and lower $\Delta\mu$(Ga), we found the ε_3 structure to be most stable, while the $\beta2_3$ structure becomes more favorable as $\Delta\mu$(Ga) is increased.

Another interesting finding is the emergence of the $\beta2_2$ structure in a very small range between the δ- and ε-type structures, which were not observed in the previous

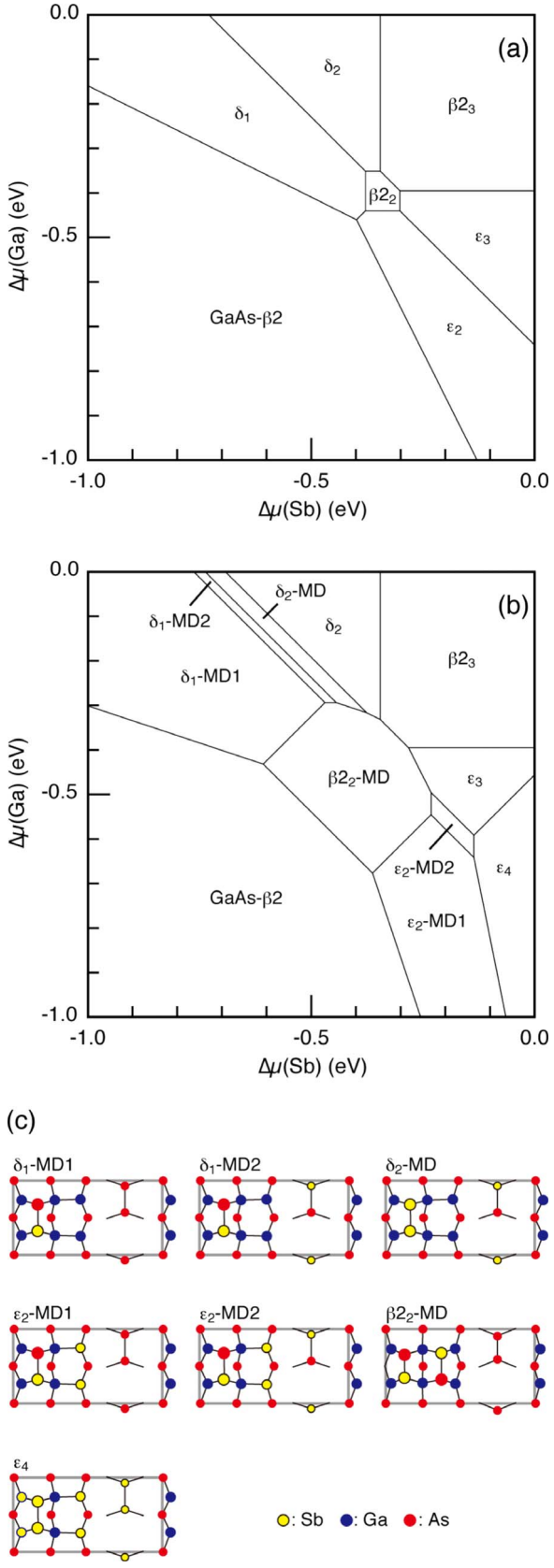

FIG. 7. (Color online) (a) Phase diagram of the Sb-induced (2 $\times$4) reconstructions versus the Ga and Sb chemical potentials. (b) Modified phase diagram including structure models with mixed Sb-As dimers shown in (c).

calculations.[5] As mentioned earlier, our STM observations have revealed that the δ- and ε-type structures emerge at low and high Sb coverages, respectively, and $\beta 2$-type unit cells are locally observed at an intermediate stage [Fig. 4(c)]. If we assume that the experimentally observed $\beta 2$-type feature corresponds to the $\beta 2_2$ structure, we can explain why the $\beta 2$-type feature is observed only in the limited range. However, it remains an open question why the (2×4) surfaces mainly consisting of $\beta 2$-type features were not observed experimentally.

In order to obtain further experimental supports for the δ_1 [Fig. 6(a)] and ε_3 [Fig. 6(b)] models, we performed RHEED rocking-curve analysis based on dynamical diffraction theory. RHEED rocking-curves were measured using the extended beam rocking facility (Staib, EK-35-R and k-Space, kSA400). The energy of the incident-electron beam was set at 15 keV. Integrated intensities of the 17 spots, (0 0), $(0\pm\frac{1}{4})$, $(0\pm\frac{2}{4})$,…, $(0\pm\frac{10}{4})$, $(0\pm\frac{11}{4})$, and (0 ± 2) for the $[1\bar{1}0]$ direction, and 5 spots, (0 0), ($\pm$1 0), and ($\pm$2 0) for the [110] direction, were used in a structure analysis. Averaging of the symmetry-equivalent spots led to nine and three independent rocking curves for the $[1\bar{1}0]$ and [110] directions, respectively. RHEED intensities were calculated by the multislice method proposed by Ichimiya.[18] 24 fractional-order and 9 integer-order reflections were used for the calculation along the $[1\bar{1}0]$ direction, and 9 integer-order reflections were used for the [110] incidence azimuth. Since, as can be seen in Fig. 5, two adjacent (2×4) units along the $[1\bar{1}0]$ direction are often oriented in the opposite directions, the calculation for the $[1\bar{1}0]$ incidence assumed the existence of two types of units. On the other hand, fractional-order reflections in the [110] direction are excluded in the present calculations, as in the case for the As-stabilized GaAs(001) $-(2\times4)$ surface,[19] because extended streaks are observed in the half-order positions, which is ascribed to the formation of one-dimensional disorder boundaries on the (2×4) surface.

Fourier coefficients of the crystal potential for elastic scattering were obtained from the atomic scattering factors for free atoms calculated by Doyle and Turner.[20] A correction due to condensation was made to fit the positions of bulk Bragg peaks at large glancing angles. For instance, the resulting mean inner potential of bulk GaAs was 13.6 eV. The correction was also applied for Sb. The adsorption of electrons in a crystal (inelastic scattering processes) is given phenomenologically by an imaginary potential, which was assumed to be 12% of its real part. The Debye temperatures in bulk layers were taken to be 275 and 285 K for Ga and As atoms, respectively.[21] For surface layers, we assumed reduced Debye temperatures of 180, 190, and 100 K for Ga, As, and Sb atoms, respectively. The thickness of a slice, in which scattering potential was approximated to be constant toward the direction normal to the surface, was about 0.1 Å. In order to quantify the agreement between the measured and calculated rocking curves, the R factor defined in Ref. 22 was used. The calculated rocking curves were convoluted with a Gaussian, which has a full width at half maximum of 0.1°, corresponding to the experimental resolution.

Figures 8(a) and 8(b) show the RHEED rocking-curves measured from the GaAs(001)$-(2\times4)$-Sb surface at 600

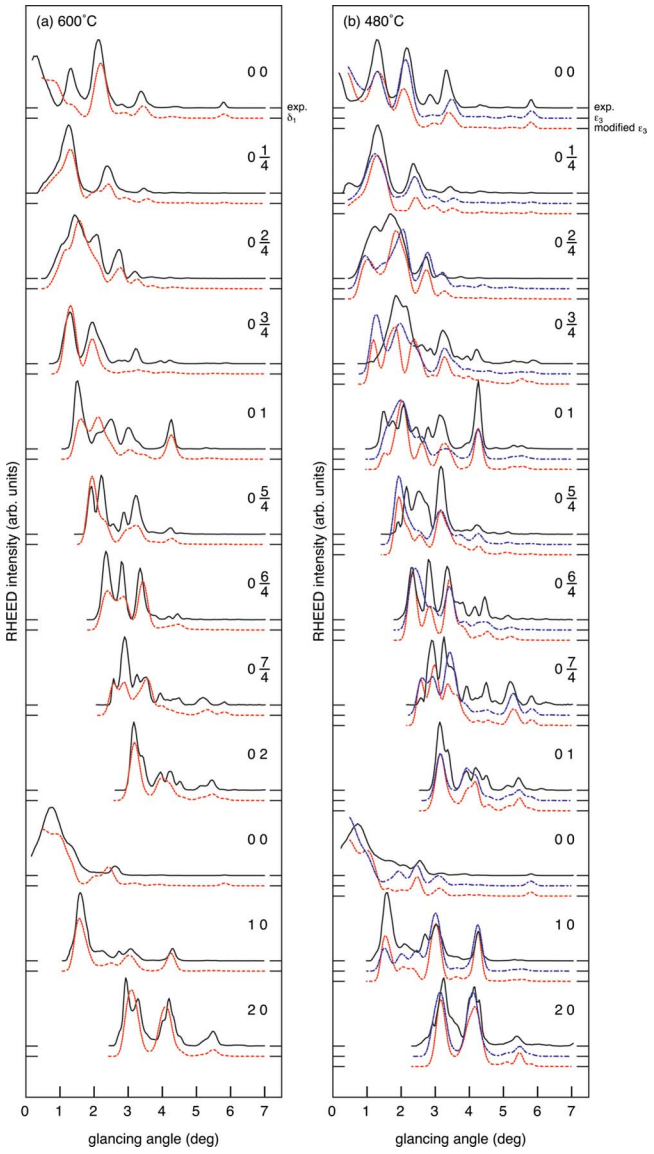

FIG. 8. (Color online) RHEED rocking curve (solid curves) measured from the Sb-induced (2×4) surfaces prepared at 600 °C (a) and 480 °C (b). The dashed curves in (a) are calculated using the atomic coordinates obtained by first-principles calculations for the δ_1 model, and the dashed and dash-dotted curves in (b) are calculated from the ε_3 and modified ε_3 models, respectively.

and 480 °C, respectively, together with the calculated ones from the δ_1 [dashed curve in (a)] and ε_3 [dash-dotted curve in (b)] models. We also measured RHEED rocking curves after the sample was cooled to room temperature, and confirmed that most of features in the rocking curves are preserved for both samples, except for the increase in the peak intensities due to the suppressed thermal vibrations. This is in good agreement with the RDS results. The atomic coordinates used for the RHEED analysis were fixed at those obtained by first-principles calculations. For the Sb-deficient (2×4) surface prepared at 600 °C [Fig. 8(a)], the majority of features in the measured rocking curves are well reproduced by the calculations (R factor=0.18) for the δ_1 model. On the other hand, for the Sb-rich ε_3 model, only modest agreement between the measured and calculated curves was achieved (R factor=0.28) [Fig. 8(b)]. However, as we will show below, the agreement is significantly improved, when the second-layer Sb and third-layer As atoms in the ε_3 model are interchanged.

TABLE I. R factors for the modified $\varepsilon_3(2\times4)$ models in which the first-(A), second-(B), and third-layer (C) Sb atoms are interchanged with third-layer As atoms.

Notations in Fig. 6(b)		
Sb	As	R factor
	a and a′	0.44
A	b and b′	0.47
	c and c′	0.48
	a and a′	0.20
B	b and b′	0.30
	c and c′	0.22
	a and a′	0.36
C	b and b′	0.38
	c and c′	0.40

RHEED intensities were calculated for the modified $\varepsilon_3(2\times4)$ models in which the first-(A), second-(B), and third-layer (C) Sb atoms are interchanged with third-layer As atoms (a, a′, b, b′, c, and c′), as indicated in Fig. 6(b). At this stage of the analysis, atomic coordinates were fixed at those for the ε_3 model obtained by the first-principles calculations. Only when the second-layer Sb atoms [B in Fig. 6(b)] are interchanged with the third layer As atoms [a, a′, c, and c′ in Fig. 6(b)], was the R factor significantly decreased, as shown in Table I. Here, we note that the difference between the a and a′ sites is not ascertained in the present analysis, because of the following reasons: (i) fractional-order reflections in the [110] direction are excluded in the present calculations, as mentioned earlier. (ii) For $[1\bar{1}0]$ direction, only structure parameters projected on the $(1\bar{1}0)$ plane are available.

Shown by dashed curves in Fig. 8(b) are the calculated RHEED rocking curves from the modified ε_3 model in which the second-layer Sb atoms [B in Fig. 6(b)] are interchanged with third-layer As atoms [a and a′ in Fig. 6(b)]. After the structure optimization by first-principles calculations, the agreement between the experiment and calculation is further improved (R factor=0.18).

The present RHEED analysis suggested six atomic geometries for the modified ε_3 structure, as shown in Figs. 9(b)–9(g). However, these modified ε_3 structures become unstable with respect to the ε model [Fig. 9(a)], as indicated in Fig. 9. While further studies are needed to resolve the disagreement, the random distribution of Sb atoms at the third layer might lower the energy of the modified ε_3 structure. On the other hand, recent x-ray diffraction measurements have shown that Sb atoms are incorporated in the fourth and deeper layers in the Sb-adsorbed GaAs(001)$-(3\times1)$ structure.[23] Thus, it is possible that the diffusion of Sb into deeper layer also occurs in the Sb-induced (2×4) reconstruction.

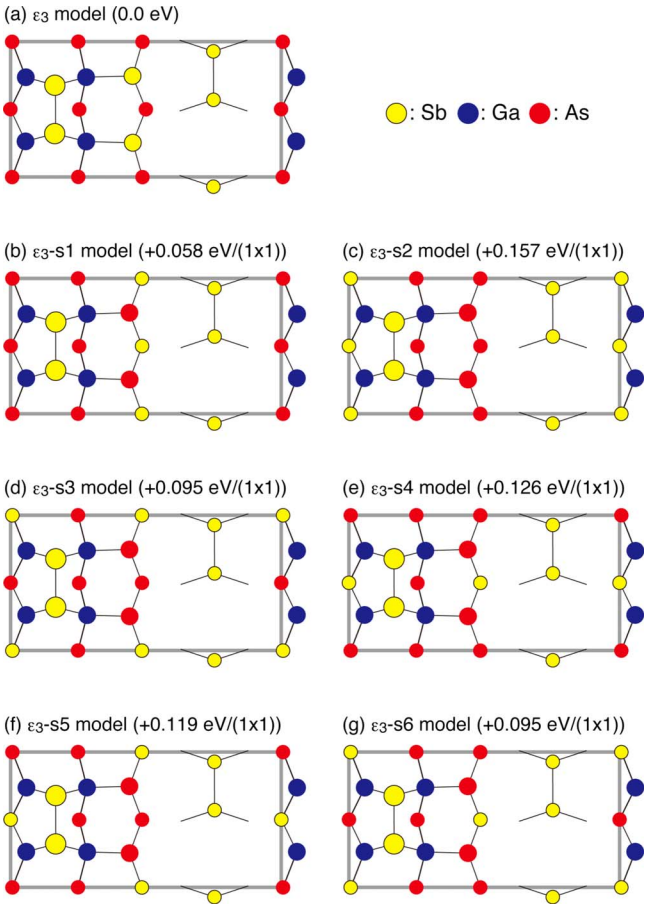

FIG. 9. (Color online) Possible atomic geometries for the modified ε_3 model. The modified models have energies higher by 0.058 eV (a), 0.157 eV (b), 0.095 eV (c), 0.126 eV (d), 0.119 eV (e), and 0.095 eV (f) per (1×1) unit cell relative to the ε_3 model.

Recent photoemission studies[7] have suggested that the Sb-induced (2×4) surface prepared at a high temperature of 550 °C contains Sb atoms at the third layer (δ_2 structure). On the other hand, the present results show that the Sb-induced (2×4) surface prepared at temperatures higher than 550 °C (e.g., 600 °C) has the δ_1 structure. This suggests that a slight difference in the substrate temperature results in different dimer species in the δ-type structure. Further interesting results were obtained when the possible existence of mixed Sb-As dimer in δ-type structures was assumed. As shown in Fig. 7(b), three variants of the δ_1 structure, δ_1-MD1, δ_1-MD2, and δ_2-MD [Fig. 7(c)] emerge for lower $\Delta\mu$(Sb) and higher $\Delta\mu$(Ga). Similar mixed dimer structures have been proposed for Bi-induced reconstructions on GaAs(001) (Ref. 24) and InP(001) (Ref. 25) surfaces. It is clearly seen that the Sb coverage in the δ-type structure is increased as $\Delta\mu$(Sb) is increased. The energies of δ-type structures are nearly degenerate in the regions where the δ_1-MD2 and δ_2-MD structures are most stable: the differences in the formation energy are below 0.03 eV/(1×1). While Sb-As, Sb-Sb, and As-As dimers are hardly distinguished in STM images, RHEED rocking curves calculated from these models are in good agreement with the experiments: the R factors are comparable with the value of δ_1 structure ($R\sim0.19$). Thus, we cannot exclude the possibility that the δ-type structure changes its dimer species depending on the preparation conditions.

The energetics of Sb-As dimers in the ε- and β-type structures have been also examined. As shown in Fig. 7(b), several structures, ε_2-MD1, ε_2-MD2, and $\beta2_2$-MD [Fig. 7(c)], emerge in the phase diagram. In addition, the ε_4 structure (Sb coverage=1 ML) is found to be most stable at the lower limit of $\Delta\mu$(Ga) and higher limit of $\Delta\mu$(Sb). However, our RHEED rocking curve analysis show that these structure models do not reach a level of satisfactory agreement with the experiments ($R>0.32$).

V. CONCLUSIONS

We studied the atomic structure of the Sb-induced (2×4) surface reconstruction on GaAs(001). We found that Sb-induced (2×4) surface changes its structure and composition depending on the substrate temperature. Structure identification based on the RHEED, XPS, and STM results revealed that the (2×4) units consisting of single anion dimer at the outermost surface layer is dominant in the whole range of substrate temperature. The (2×4) structure with low Sb coverage has δ-type structure. For the Sb-rich (2×4) phase, we proposed the structure model consisting of anion dimers at the first and third layers and three-coordinated As atoms at the second layer (ε-type structure). Our first-principles calculations suggest that Sb-Sb, As-As, and Sb-As dimers coexist in the Sb-induced (2×4) reconstructions, their relative densities being sensitive to the preparation conditions.

ACKNOWLEDGMENT

We are indebted to T. Hanada for use of the RHEED intensity calculation program.

*Author to whom correspondence should be addressed; ohtake.akihiro@nims.go.jp

[1] F. Maeda, Y. Watanabe, and M. Oshima, Phys. Rev. B **48**, 14733 (1993).
[2] F. Maeda and Y. Watanabe, Phys. Rev. B **60**, 10652 (1999).
[3] M. Sugiyama, S. Maeyama, F. Maeda, and M. Oshima, Phys. Rev. B **52**, 2678 (1995).
[4] N. Esser, A. I. Shkrebtii, U. Resch-Esser, C. Springer, W. Richter, W. G. Schmidt, F. Bechstedt, and R. Del Sole, Phys. Rev. Lett. **77**, 4402 (1996).
[5] W. G. Schmidt and F. Bechstedt, Phys. Rev. B **55**, 13051 (1997).
[6] P. Moriarty, P. H. Beton, Y.-R. Ma, M. Henini, and D. A. Woolf, Phys. Rev. B **53**, R16148 (1996).
[7] P. Laukkanen, R. E. Perälä, R.-L. Vaara, I. J. Väyrynen, M.

Kuzmin, and J. Sadowski, Phys. Rev. B **69**, 205323 (2004).
[8] T.-L. Lee and M. J. Bedzyk, Phys. Rev. B **57**, R15056 (1998).
[9] L. J. Whitman, B. R. Bennett, E. M. Kneedler, B. T. Jonker, and B. V. Shanabrook, Surf. Sci. **436**, L707 (1999).
[10] A. Ohtake, Surf. Sci. Rep. **63**, 295 (2008).
[11] S. Gopalan, P. Lautenschlager, and M. Cardona, Phys. Rev. B **35**, 5577 (1987).
[12] M. D. Pashley, Phys. Rev. B **40**, 10481 (1989).
[13] We also carried out the calculations for the δ- and ε-type structures with the As-As and Sb-As dimers at the first layer, and confirmed that such structures also reproduce the observed STM features.
[14] P. Hohenberg and W. Kohn, Phys. Rev. **136**, B864 (1964).
[15] D. Vanderbilt, Phys. Rev. B **41**, 7892 (1990).
[16] J. Yamauchi, M. Tsukada, S. Watanabe, and O. Sugino, Phys. Rev. B **54**, 5586 (1996).
[17] J. P. Perdew, K. Burke, and M. Ernzerhof, Phys. Rev. Lett. **77**, 3865 (1996).
[18] A. Ichimiya, Jpn. J. Appl. Phys., Part 1 **22**, 176 (1983); A. Ichimiya, *ibid.* **24**, 1365 (1985).
[19] A. Ohtake, M. Ozeki, T. Yasuda, and T. Hanada, Phys. Rev. B **65**, 165315 (2002); A. Ohtake, M. Ozeki, T. Yasuda, and T. Hanada, *ibid.* **66**, 209902(E) (2002).
[20] P. A. Doyle and P. S. Turner, Acta Crystallogr., Sect. A: Cryst. Phys., Diffr., Theor. Gen. Crystallogr. **24**, 390 (1968).
[21] U. Pietsch and N. K. Hansen, Acta Crystallogr., Sect. B: Struct. Sci. **52**, 596 (1996).
[22] T. Hanada, H. Daimon, and S. Ino, Phys. Rev. B **51**, 13320 (1995).
[23] T. Kaizu, M. Takahasi, K. Yamaguchi, and J. Mizuki, J. Cryst. Growth **310**, 3436 (2008).
[24] M. P. J. Punkkinen, P. Laukkanen, H.-P. Komsa, M. Ahola-Tuomi, N. Räsänen, K. Kokko, M. Kuzmin, J. Adell, J. Sadowski, R. E. Peräla, M. Ropo, T. T. Rantala, I. J. Väyrynen, M. Pessa, L. Vitos, J. Kollár, S. Mirbt, and B. Johansson, Phys. Rev. B **78**, 195304 (2008).
[25] A. Z. AlZahrani and G. P. Srivastava, Phys. Rev. B **79**, 125309 (2009).